MEASUREMENT OF BUBBLE SIZE DISTRIBUTION IN FLOTATION FROTHS

Eric M. Tshibwabwa and Micheal H. Moys

School of Chemical and Metallurgical Engineering, University of the Witwatersrand, Private Bag 3, Johannesburg, WITS 2050, South Africa

Clayton. Bhondayi

Material and Process Synthesis, University of South Africa, Florida, South Africa

ABSRACT

Most valuable products produced by flotation pass through the froth phase of the flotation process. Most research into flotation has however been focused on the pulp phase. The froth phase has attracted more research in recent times. The complex processes that occur in the froth phase – detachment, re-attachment, coalescence of bubbles, and competition for attachment sites, mixing and transport all combine to affect the net transfer of mineral particles into the concentrate.

A variable which has significant influence is the bubble size distribution (FBSD) in the froth phase. Bubbles are formed at different sizes in the pulp phase and coalesce at different rates and as a result the bubble size distribution varies from point to point in the froth phase. Substantial coalescence gives rise to loss of bubble surface area and hence loss of recovery. Competition for attachment sites gives rise to an increase in grade.

No method for measuring froth bubble size distribution (FBSD) was available until Bhondayi and Moys developed a method for measuring chord lengths in the froth using a probe dropped at known velocity through the froth. The average of these chord lengths was assumed to be a proxy for FBSD; this was calibrated using FBSD measured in the laboratory using photographs taken through the transparent wall of a laboratory cell.

In this paper we discuss the application of stereological techniques to obtain estimates of the actual FBSD. These are calibrated using the above-mentioned photographic technique. They are then used to quantify the effect of froth depth and frother concentration on the FBSD in a semi-batch laboratory cell and a continuous Mintek pilot plant.

KEYWORDS

Froth phase, Intra-bubble impact distance, Froth bubble size, froth height, frother dosage, model

INTRODUCTION

Froth flotation is a method for selectively separating a valuable mineral from waste materials by means of the air bubbles dispersed in pulp phase. The flotation process is widely used for upgrading valuable minerals in the field of mining. Hundred diverse minerals, including most of the world's nickel, copper, zinc, cobalt and lead are processed by the flotation process (Wei Zhang, 2009). It has also been stated by Seungwoo Park (2009), the flotation process has been used to remove the contaminant compounds from waste water in the water treatment industries, ink removal from paper fibres in the paper industries as well as the bitumen oil sands in the petroleum industries. The hydrophobic particles are truly recovered as concentrate, if the attachment of bubble-particle aggregates travel the whole height of froth phase without detachment and attaining its top surface. The target is to recover all desired mineral particles from the low and high grade ores as much as possible.

During the rise of bubbles in the froth, they coalesce at different rates and as a result of the bubble size distribution varies from point to point in the froth phase. Accordingly, detachment of desired particles from bubbles in the froth take place, provoking decrease in mineral recoveries (Yianatos et al., 1986). Reattachment of desired particles can take place in the froth phase if there is availability of bubble surface area, which results in mineral upgrading (Moys, 1979). The froth phase plays an important role in the process of froth flotation, aiming to improve the grade and recovery of mineral particles.

Bubble size is one of the variables that should be controlled in the flotation process (Moys and Finch, 1988). Liu et al. (2005), reported that froth bubble size is the major feature used by the operators to assess the status of the process at the Laronde plant. The effectiveness of the flotation process is significantly related to the size of bubble distribution in the froth phase. Bubble size distribution is an indicator of complex process occurring within the froth phase (Moys, 1979). The control of froth bubble size distribution in the flotation process is expected to be relevant to flotation efficiency. It determines the surface area flux of the bubbles into the concentrate stream which determines the mineral grade and recovery. Therefore, froth bubble size needs to be controlled during the flotation process.

The complex processes occurring in the froth phase are not well understood and have not been quantified adequately yet due to the lack of adequate methods to measure froth bubble properties such as diameter, rate of coalescence etc. Many measurement techniques have been developed to measure bubble size in pulp phase. While few researches have been conducted in froth phase. Finch et al., 2004 investigated two methods based on (a) drift flux calculation and (b) capillary (UCT technique). These, have been applied in the laboratory pulp bubble size measurements. However, they present disadvantages on froth bubble size measurement, due to the complicated nature and structure of froth phase. Ata, Ahmed & Jameson (2003) performed a photographic method to estimate froth bubble size from photographs of the transparent flotation cell wall. This cannot be applied at industry scale because it requires transparent flotation cell walls to allow froth bubble photography. Murphy et al. (1996) found observing the surface of the froth is not enough. The use of surface of the froth bubble sizes has been enough for reliable and industrially applicable method to measure bubble sizes within the froth. No adequate method for measuring FBSD was available until Bhondayi and Moys 2014 developed a method for measuring chord lengths in the froth using a probe dropped at known velocity through the froth. The average of these intra bubble impact distances IIDs or chord lengths CL was assumed to be a proxy for FBSD; this was calibrated using FBSD measured in the laboratory using photographs taken through the transparent wall of a laboratory cell. In the previous work, comparison of the technique to the photographic method

indicated that the technique over-estmates the actual bubble size distributions with 31 %. This might be due to random drop of the probe and average IIDs. In this paper we discuss the application of stereological techniques to obtain estimates of the actual FBSD. These are calibrated using the above-mentioned photographic technique. They are then used to quantify the effect of froth depth and frother concentration on the FBSD in a semi-batch laboratory cell and a continuous Mintek pilot plant.

EXPERIMENTAL IID MEASUREMENT SET-UP

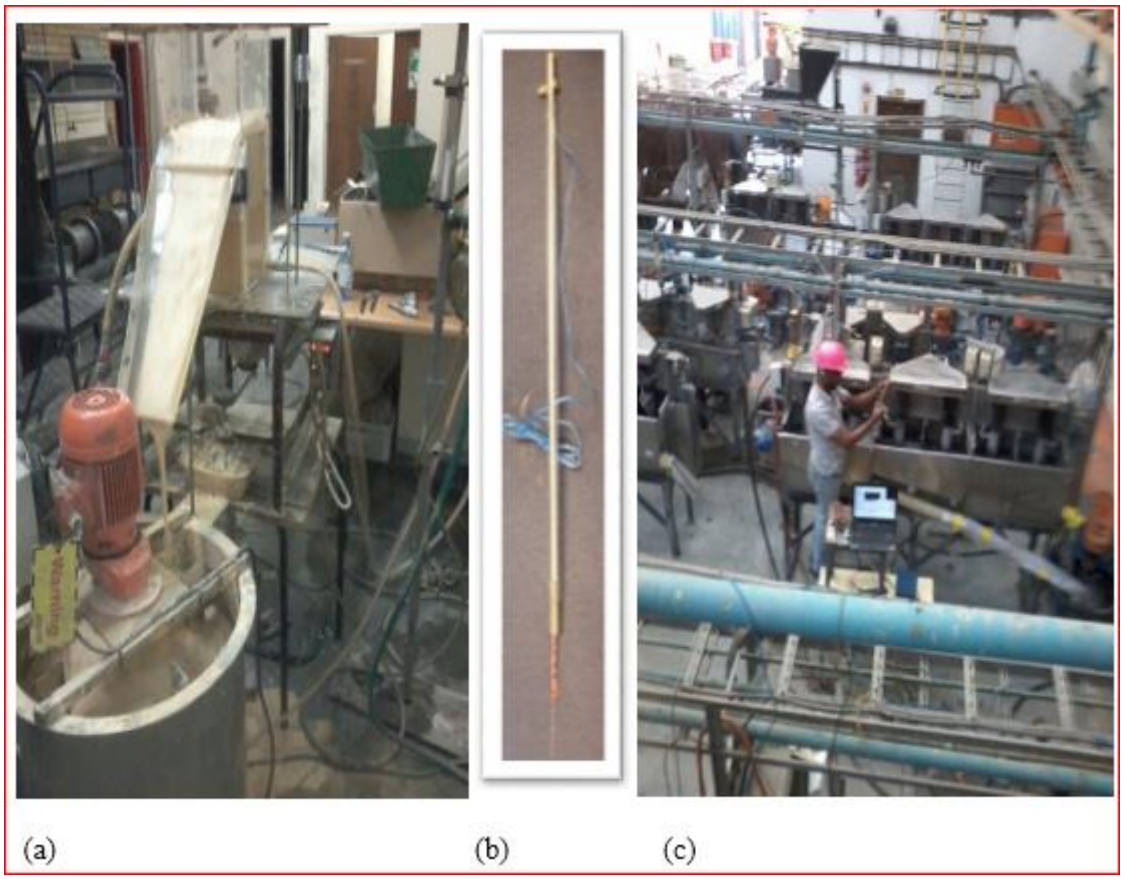


Fig. 1 Showing (a) operating Wits lab flotation cell (b) Electrical probe and (c) Mintek flotation pilot rougher cell within which froth bubble measurements were conducted.

The measurements of IIDs were conducted. Firstly, in mechanically agitated variable depth flotation cell at the University of Witwatersrand (Wits). These experiments were operated with a pulp volume of 8litres in pseudo-steady state mode by connecting it to a 100 litres mixing tank allowing both concentrate and tailings to flow back into the mixing tank as shown in Figure 1a. An artificial ore comprised of 80% silica and 20% limestone was chosen for all the experiments, it was chosen mainly because of its availability in suitable size ranges and also the fact that it can be used in a closed circuit without problems of surface oxidation (of sulphide ores). Froth depth (measured from the pulp froth interface to the concentrate launder) was set at value 7.6 cm while

average superficial gas velocity was set at 0.75cm/s. This resulted in froth height of 10.5cm. Froth height herein is defined as height from the pulp-froth interface to the surface of the froth. Agitation rate was maintained at 1200 rpm and solids concentration was maintained at 15%w/w in all experiments. Oleic acid and Dowfroth were added respectively at rate of 30 g/ton of limestone and 0.30 mg/ per liter of water.

Secondly, the measurements were carried out on liquid-gas phases in the rougher bank of the secondary flotation circuit at the Mintek pilot plant, Johannesburg, South Africa. The flotation bank has 6 rectangular cells in series (each 30 × 40 cm long) as shown in Figure 1b. The gas was injected into the impellor zone. The water level was controlled by an interface controller. The experiments were operated in closed circuit. This means that both liquid and froth streams drain back into the pump sump. It is then pumped back into the rougher bank through first cell. The water flow rate, airflow rate, liquid-froth interface and impeller speed were operated at constant values. The variable manipulated during the study was frother dosage. Three different sets of conditions were used; 3 ppm, 6ppm and 12 ppm. All changes and measurements were done on the second cell of the rougher bank.

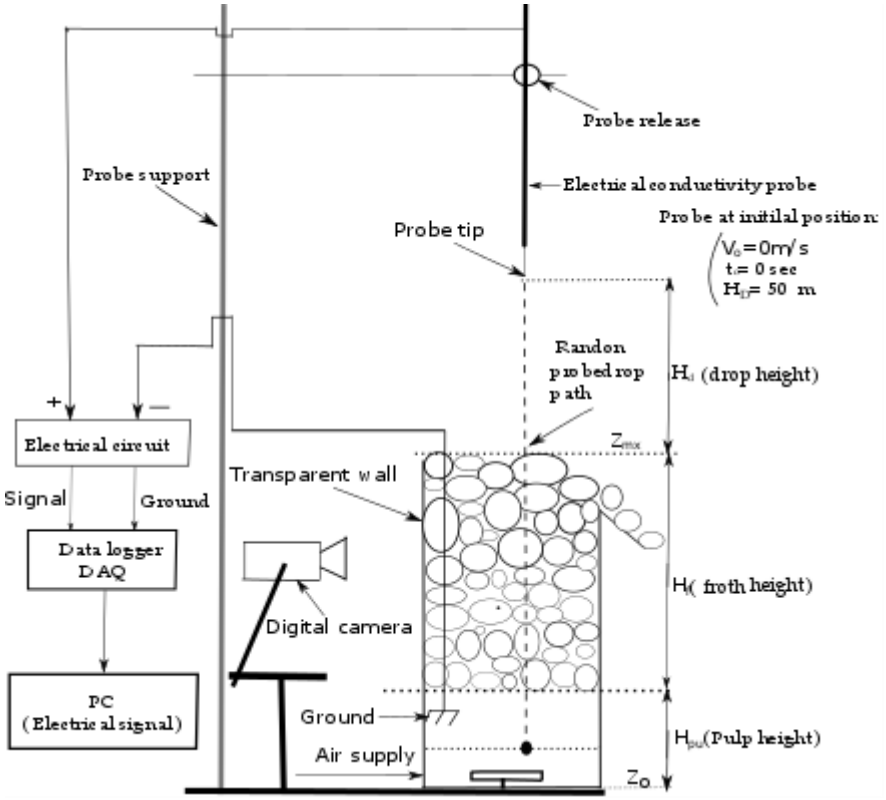


Fig. 2-Schematic of the experimental set-up to measure IID.

Measurements of IIDs or CL in both Wits lab and Mintek pilot cells were done by dropping the conductivity probe several times into the froth phase from a known height of 50 cm respectively, with 0 m/s as an initial velocity as displayed in Figure 2. Care was taken to ensure that the probe was falling vertically into the froth phase and within a fixed locus on the surface of the froth. The electrical signals were routed to a PC through an SCXI 1520 data logger set at 40kilosamples per second. The measured value of the froth height (HF) and the time it takes the probe to cut across

the froth (obtained from the output signal) were used to quantify the effect of froth resistance on probe velocity.

MATHEMATICAL MODEL

Single bubble model

The first problem that needs to be addressed is for single bubble with diameter D_i. 1) What is the positions of probe at both bubble top and bottom (i.e. entry and exit points)? 2) What is the cumulative distribution that a random drop of the probe measures an intra bubble impact distance IID having its distance less than or equal to L_j ($where\ L_j < D_i$)? 3) What is the probability density that a random drop of the probe measures an intra bubble impact distance IID having its distance between $L_j\ and\ L_{j+1}$($whereL_j\ and\ L_{j+1} < D_i$) ?

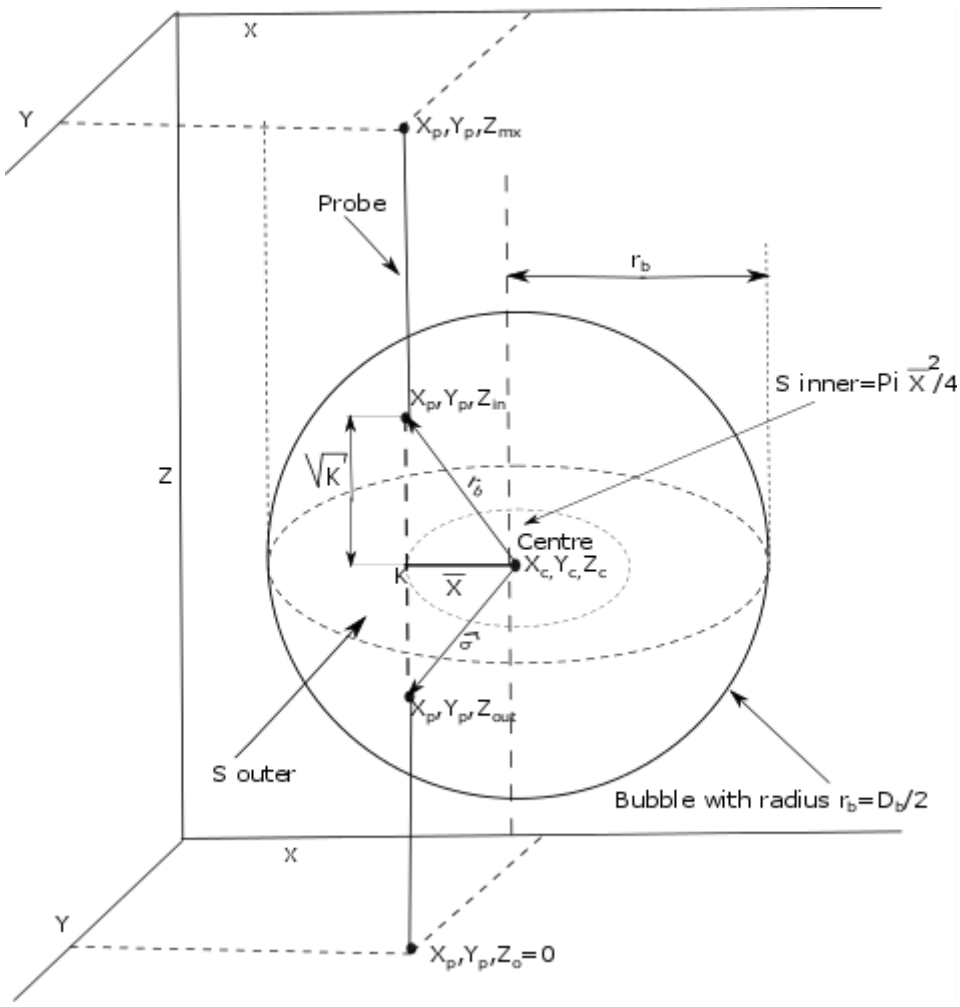


Fig.3. Representation of geometric model schematic of probe and bubble with radius r_b. Measurement of IID generated by a probe intercepting the successive points of bubble films (top and bottom)at IID of $L_b = 2\sqrt{K}$.

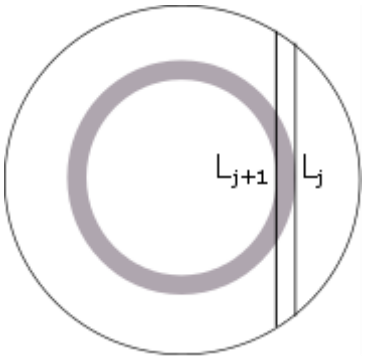


Fig.4 Representation of ring area regarded to estimate IID between L_j and L_{j+1}

Consider a cubical box which is penetrated by random vertical drop of the probe that is parallel to one of the lateral edges. Let us take a single bubble of diameter D_b or $2r_b$and with its centre coordinates X_c, Y_c, Y_c would be hit by probe as illustrated in Figure 3. It is important to note that in this method, bubble is assumed to have spherical shape. The bubble is randomly cut by probe at two successive position points,at Z_{in}, where the probe enters the bubble and Z_{out}, where the probe comes out of the bubble. The both positions of the probe Z_p can be deduced as

$$Z_{in} = Z_c + \sqrt{K} \qquad and \qquad Z_{out} = Z_c - \sqrt{K} \tag{1}$$

Where K is given by K= ${r_b}^2 - \left(X_p - X_c\right)^2 + \left(Y_p - Y_c\right)^2$. An intra bubble impact distance IID, is determined as

$$IID = L_b = Z_{in} - Z_{out} \tag{2}$$

From Figure 3, Eq.(2), can also be given as

$$IID = L_b = 2\sqrt{K} \tag{3}$$

Let us determine the cumulative distribution and probability density function which describes the way of finding an intra bubble impact distance IID,L_b for defined bubble size D_b. Supposing that a single bubble with diameter D_b, is randomly intercepted N times of drops as indicated in Figures 3. From this, we can try to find the probability of IID less than or equal to L_b. The cumulative distribution function of IID, $P(L_b)$ is defined here as the number of intra bubble impact distances IIDs less than or equal to L_b over the total number of IIDs in the bubble. It can be written as follows:

$$P(L_b|D_b) = \frac{Number\ \ of\ IIDs\ \ less\ than\ or\ equal\ to\ L_b}{Total\ \ number\ \ of\ IIDs\ in\ bubble} = \frac{Souter}{S\ bubble} \tag{4}$$

Where $S\ inner$ is the surface area of inner disk and $S\ bubble$ is the total equatorial surface area of bubble. These are well represented in Figure 3. The cumulative distribution is developed as

$$P(L_b|D_b) = 1 - \frac{S\ inner}{S\ bubble} = 1 - \frac{\pi \overline{X}^2/4}{\pi {r_b}^2/4} \tag{5}$$

The probe views a 3-D projection of the bubble in Figure 3. Considering the case of a spherical bubble with diameter D_b, the 2D projection of the bubble is a circle with the same diameter D_b. Now, it should be noted that for every point inside the circle, there is associated with it, a unique IID for which the considered point is the midpoint of the IID. Thus, choosing a random IID of a circle is equivalent to choosing a random point inside the circle. The locus of the midpoints of the IID is a circle with dimensions as shown in Figure 3. Any point on the bubble surface area corresponds to an IID with length L_b and every IID with length L_b will have its midpoint on the circle. For a IID whose distance is between L_j and L_{j+1}, it is necessary that its midpoint should lie in the shaded area as a given in Figure 4. The probability that the probe tip intercepts a bubble at distance $\overline{X}$ from bubble center can be modelled, once probe tip position and bubble geometries are known as displayed in Figure 3. Once the probe tip and bubble are geometrically defined, Pythagoras relationship relating the IID to the position of the probe with regards to bubble centre can be used. From Eq.(2), $\overline{X}$ can be found by Pythagoras using Figure 3 given as

$$\overline{X} = \left[{r_b}^2 - \left(\sqrt{K}\right)2\ \right]^{0.5} \qquad (6)$$

Substituting Eq.(6) into Eq.(5), we obtain:

$$P(L_b|D_b) = \frac{{L_b}^2}{4\,{r_b}^2} = \frac{{L_b}^2}{{D_b}^2} \qquad for\ \ 0 < L_b < D_b \qquad (7)$$

Where Eq.(7) is the cumulative distribution function of IID, L_b is the IID and D_b is the bubble diameter. The IIDD density function for a single bubble calculated as

$$p_j(L_j) = \sum_i p_{ij}\left(L_j, D_i\right) \qquad (8)$$

The probability of the drop of the probe measures an IID with distance between $L_j\ and\ L_{j+1}$ $\left(L_j\ <\ L_{j+1}\right)$ can be calculated as:

$$p(L_b|D_b) = P\left(L_{j+1}\middle|D_i\right) - P\left(L_j\middle|D_i\right) \qquad (9)$$

Where $p(L_b|D_b)$ is the probability that probe measures an IID between $L_j\ and\ L_{j+1}$. Hence for known size distribution, we can calculate a probability of IID class for each diameter class using Eq.(9).

FBSD to IIDD

FBSDs and IIDDs are typically represented in the form of histograms. The entire relevant class of the froth bubble size hit by drop of the probes is divided into discrete "classes." The class sizes, typically, are proposed to be uniform which begins from the first class, depending on how the measurements were conducted or what assumption was adopted. The histogram plots the number of bubbles measured by a probe, as is applicable in this work that are recorded in each of these classes.

IIDDs for a population of bubbles with equal size. The histogram for the BSD of a group of bubbles is represented by a single class. The location of the rectangular corresponds to the class representing the size of the bubble with equal size. In a discretized form, the value of the class size will be unity. The classes are assumed to be uniformly sized having width equal to ΔD , $\Delta D =$

D_{mx}/M and the domain considered extending from 0 to D_{mx}. It is useful to define a representative size, wherein, each bubble contained in the class can be assumed to be of the corresponding representative size. In this model, the bubble size here was taken as the average $\overline{D}_i$ of minimal and maximal boundaries $\overline{D}_i = [D_i + (D_i + \Delta D)]/2$. This is done so as to make the calculations more lucid and as will be demonstrated later by extensive validation, it does not affect the model applicability. The classes are constructed from the smaller to larger sizes. In the previous section, the problem of determining the probability of measuring the IID less than or equal to specific distance and the probability of measuring an IID within a particular size range with boundaries $L_j \; and \; L_{j+1}$. Now the number of bubble is significant, the cumulative and probability obtained for a single bubble can be applied to the fraction of the total number of bubbles that can be measured an IID less than or equal to L_j and can be measured as distance between sizes $L_j \; and \; L_{J+1}$. In this work, it is expected that the number of bubbles or/and IIDs recorded by the drop of the probe is sufficiently large enough to obtain accurate size distribution.

Let the fraction of the total bubbles that contained in the i^{th} class estimated as having a specific IIDs of distance L_j, be denoted by $P(L_j|\overline{D}_i)$. As defined in the previous section, the probability of measuring an IID in the j^{th} class with minimal and maximal boundaries for a bubble belonging to the i^{th} class can be written as $p(L_j|\overline{D}_i)$. Let the number of the bubbles in the i^{th} class be M_i and represented by size $\overline{D}_i$ and the total number of bubbles measured by a probe be N_T . Theoretically, the probability density function of intra bubble impact distance from Wits bubble sizer, $p(L_i)$, can be described by the equation:

$$p(L_i) = N_T \int_0^{\infty} p(L_j|D_b)p(D_b)dD_b \qquad (10)$$

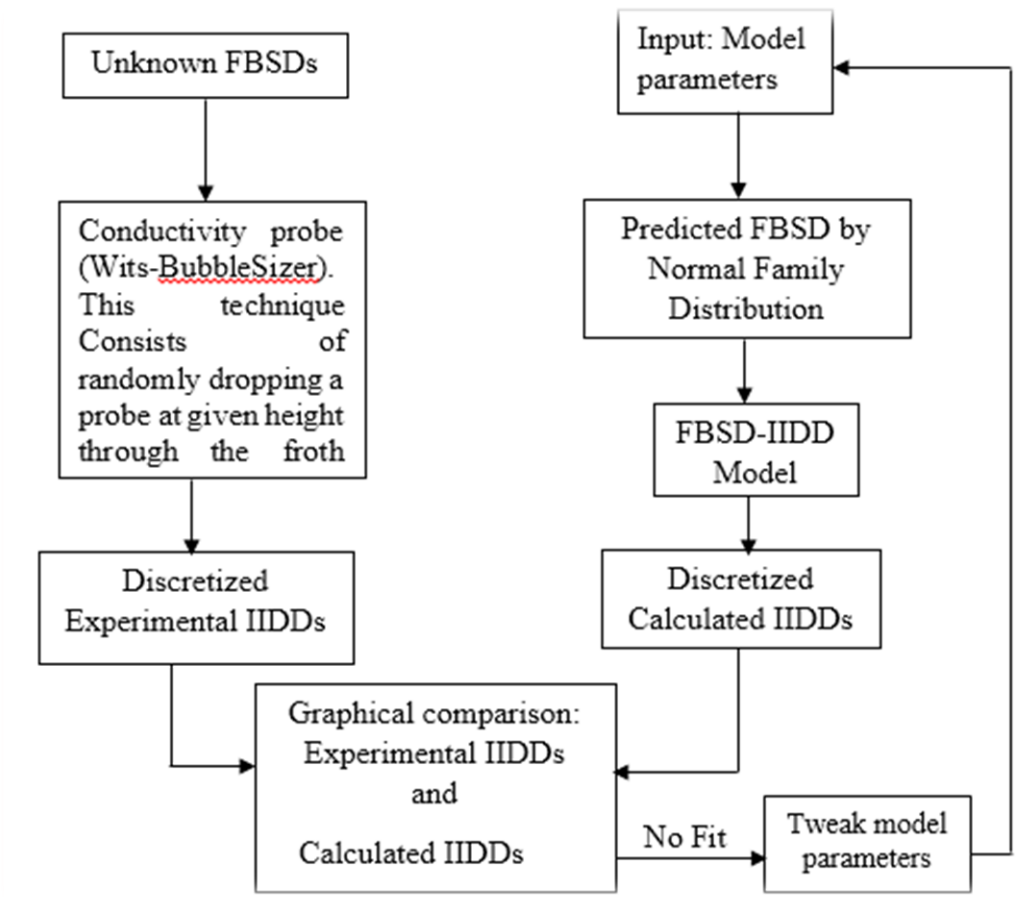
Where $p(L_j|D_b)$ is the conditional probability density function of obtaining an IID of size L_i from the bubble with size D_b. M number of classes with width ΔD and midpoint sizes $\overline{D}_{1,\ldots\ldots,M}$ can be generated within the assumed size range of $p(D_b)$. The intra bubble impact distance IIDD from the probe technique can then be approximated by

$$p(L_j) = M_i \sum_{j=1}^{M} p(L_j|\overline{D}_i)p(D_i)\Delta D \qquad (11)$$

Thus, Eq.(11) can be served to calculate the intra bubble impact distance IIDD in the j^{th} class for a population of bubbles. It is reasonable to assume that the bubbles have different probability to be hit by the drops of the probe. Large bubble is more likely hit by the probe.

Procedure for determining of bubble size distribution

A general analytical solution to Eq.(11) does not exist, although this is possible for some special cases (Liu and Clark, 1995). A numerical procedure is then adopted to approximate the integral in Eq.(10). Many methods are proposed to invert the transform problem of calculating the particle size distribution from chord length distribution (Li et al., 2005; Worlistschek et al., 2005). In this work, two methods are proposed to determine the estimates of bubble size distributions.



Good Fit implies goodest of pars

Figure 5. Bloc diagram showing the model algorithm to determine BSDs from IIDDs measurement using Wits Bubble-sizer.

Firstly, an interactive method beginning with predicting the BSD. Typically, the size of bubbles or particles can follow a normal distribution or lognormal distribution, $p(D_b)$ with two parameters μ an δ (Matsuura, 1984; Jillavenkatesa, 2001). A predicted bubble size distribution BSD, can be calculated as

$$p(D_i) = \frac{1}{\sigma\sqrt{2\,\pi}} e^{-(D_i-\mu)^2/2\delta^2} \qquad (12)$$

The corresponding IIDD is calculated using BSD-IIDD model as described in the previous section. In Eq.(12), μ is the average diameter and δ is the standard deviation. In this method, these two parameters can be optimized using a least-squares method such that the solution of Eq.(11) gives a $P_{Cal}(L_j)$ that closely matches the experimental intra bubble impact distance distribution IIDDs obtained from the drop of the probe, $p_{Meas}(L_j)$. The sum square error SSE between the calculated IIDDs and the experimental measured IIDDs is minimized through μ, δ using "SOLVER tool" represented by the equation

$$\Psi(\delta,\rho)=\sum_{j}^{N}\left[P_{Cal}(L_j)\ -P_{Meas}(L_j)\ \right]^2 \qquad (13)$$

Where Ψ is the sum of the error squares (SSE), $P_{Meas}(L_j)$ is the experimental measured IIDD, $P_{Cal}(L_j)$ is calculated from model, $\mu\ and\ \delta$ are fitting model parameters average diameter and standard deviation, respectively. This approximation would require the size range of the bubble size distribution $p(D_b)$. Since $p(D_b)$ is unknown, a size range wide enough to cover the entire $p(D_b)$ will need to be assumed. One approach is to assume that the size range of $p(D_b)$ is the same as that of $p_{ex}(L_j)$. If the sample size is large, $p_{ex}(L_j)$ will indeed cover a wider size range than the $p(D_b)$.

Secondly, the BSD is also proposed to be obtained by Inversion matrix. The Eq.(11) can also be computed in the following matrix form

$$[\mathrm{L}]=[A_{ij}][\mathrm{D}]\ \Delta\mathrm{D} \qquad (14)$$

The overall IIDD for a population of bubbles may be obtained by summing the IIDD in each class in the IIDD. Eq.(11) can be applied in the i^{th} class for a general BSD. The bubble size distribution BSD is also proposed to be obtained by Inversion Matrix. For the backward calculation of the BSD from the IIDD,$[L]$, which is given by the experimental data, the probability density distribution, $[D]$, can be computed via the Inversion matrix as

$$[D]=\left[A_{ij}\right]^{-1}[L] \qquad (15)$$

Where the inversion matrix $[A]^{-1}$ can be obtained directly for $M=N$. However, for the case of $M\neq N$, a singular value decomposition (SVD) algorithm must be used to compute pseudo-inverse of non-square matrix.

It is noted that the choice of N and M would affect the solution accuracy and overall computational time. It is found that a minimum N of 20 is needed to obtain a reasonable solution. Technically, $p(D_i)$ does not need to follow a particular distribution function. However, the optimization problem arises especially when the number of classes, M, in $p(D_i)$ is large. Nonetheless, the type of probability distribution function used can still be specified depending on the system and the specific application.

RESULTS AND DISCUSSION

The methodology proposed in this study was first validated for froth bubbles as a function of froth height in a lab transparent flotation cell. Froth bubbles were calibrated using FBSD measured in the laboratory using photographs taken through the transparent wall of a laboratory cell.

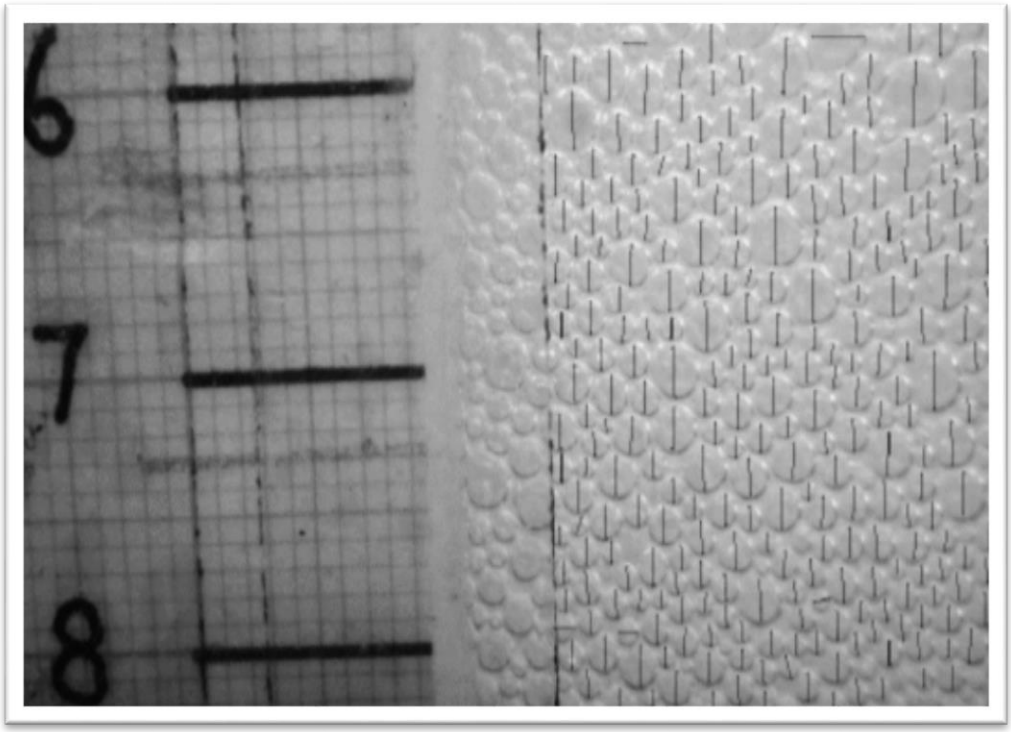


Fig. 6: Illustration of manual bubble size measurement using ImageJ with lines indicating measured diameters

It is considered that froth bubbles are spherical based on image of froth bubbles as illustrated in Figure. 6. The images captured by the digital camera, FBSD was prepared for measurement of the sauter mean diameters from image analysis. A probability density of FBSD, found by summing up the size class distributions, was regarded as the FBSD of the sample. The probability density was then discretized by dividing the total number of bubbles in order to facilitate comparison with the predicted FBSD. The discretized FBSD is displayed in Figure 8a and 8b as a function of froth height 2 cm, 4 cm, 6 cm, 8 c, and 10.5 cm from the pulp-froth interface. FBSDs were obtained through image analysis performed on a different number of 87, 129, 234,276 and 345 bubbles in froth segments 0-2, 2-4cm, 4-6, 6-8 and 8-10.5 cm with width 2 cm. The corresponding IIDDs were also known in each segment. The IIDDs were also discretized by dividing the IIDDs by the total number of IIDs measured. The present model was applied to invert the FBSD from the measured IIDD in each froth segment. A normal distribution was employed to predict the FBSD in each froth segment. Uniform class size of 0.11 mm with total interval of 0-10 mm was corresponding to the type of data available from FBSD-IIDD measurements. The distributions regarded were discretized by dividing with regard to total number of froth bubbles or IIDs, as was important to facilitate comparison. Two parameters values, average and standard deviation, for predicting the FBSD were found by matching the discretized IIDD found from the present model with the discretized measured data using the drop of the probe (Wits Bubble-sizer). A graphical comparison between the two is displayed in Figure 8c and 8d, respectively probability density and cumulative distribution functions. The optimal model parameters (μ, δ) using model algorithm, 1.21 and 0.24; 1.65 and 0.301; 2.2 and 0.351; 2.75 and 0.401; 3.3 and 0.501 were obtained to offer the sum square error values 0.12, 0.23, 0.26, 0.46 and 0.53 for the match in froth height FH respectively from top surface to froth-pulp interface. The sum square error values found are

significant low. As can be observed from the Figure 8c and 8d, there is a sufficient fit between the model-predicted IIDD and the experimental measured IIDD in all ranges of sizes. The comparison between the discretized FBSD measured experimentally and the discretized FBSD using the model displayed in Figure 8a. As may be observed this in Figure, the model precisely predict the FBSD using just the IIDD information. Comparison of the results from the actual FBSD and inversion matrix for a normal distribution is shown on Figure 8b. It is observed from the figure, the retrieved FBSDs obtained with inversion matrix, are in reasonable agreement with the measured actual FBSD inversion matrix. The retrieved FBSDs noticed from figure are nearly the same.

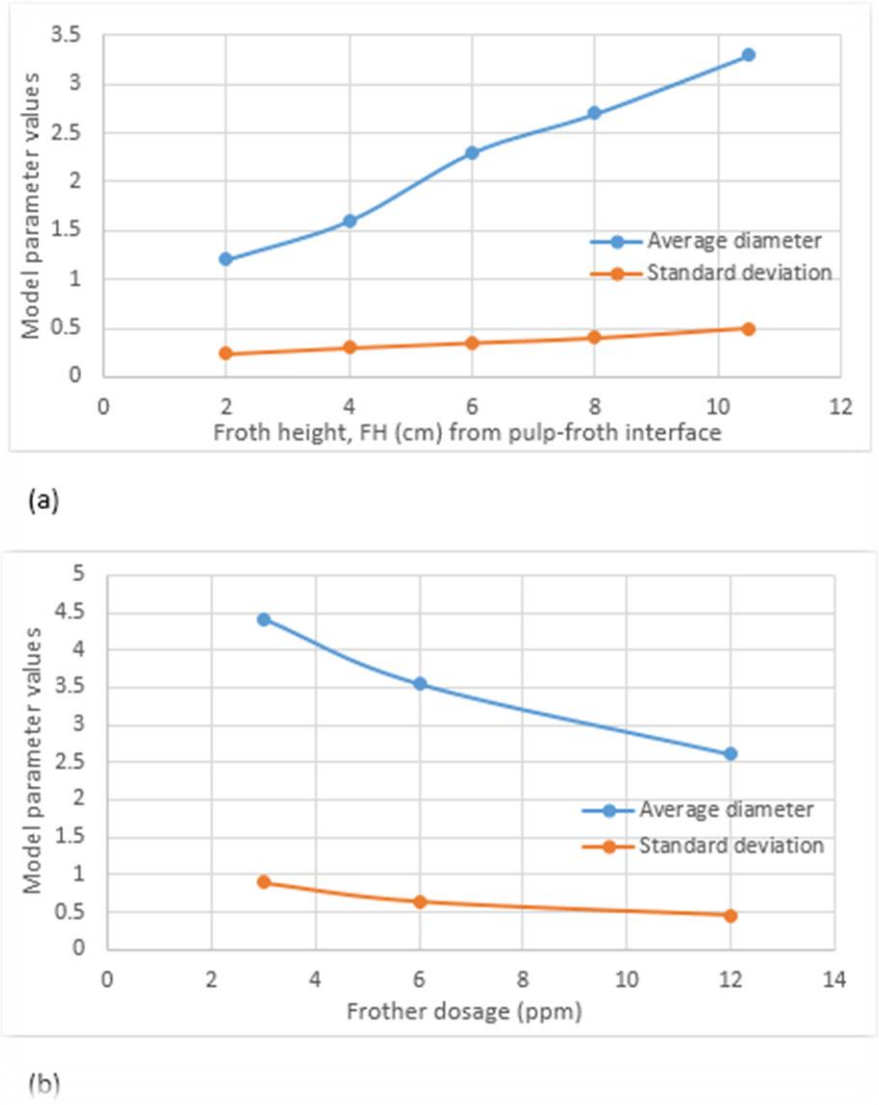


Fig. 7 Model parameters as a function of (a) froth height and (b) frother dosage

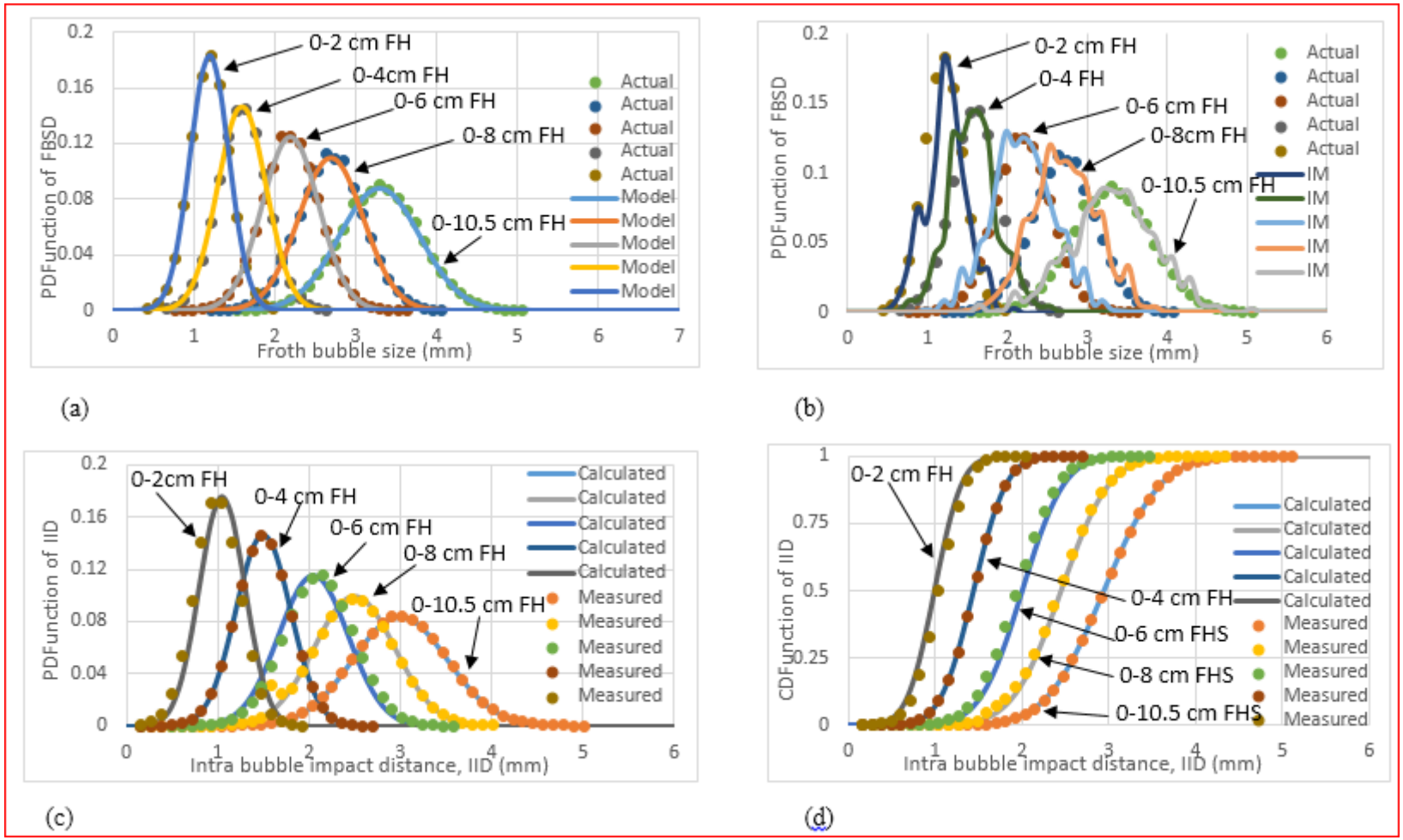


Fig.8 (a) Comparison of the model-predicted FBSD with photographic actual FBSD (b) Comparison of the Inversion matrix, IM with photographic actual FBSD (c) and (d) Comparison between model-calculated IIDDs with experimental measured IIDDs as function of froth height, respectively, PDF and CFD.

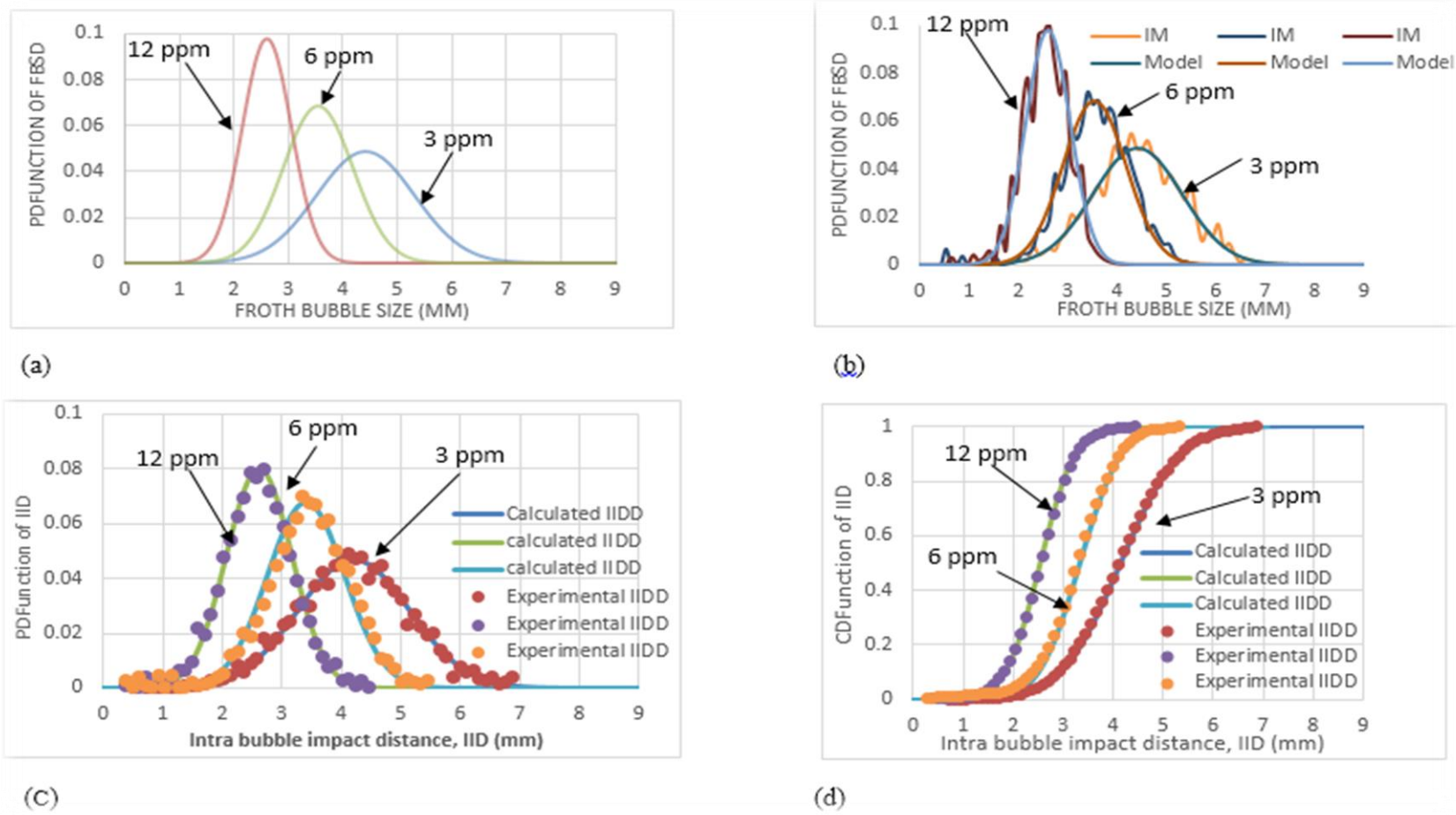


Fig.9 (a) Estiamtion of FBSD from measured IIDD as function of frother dosages, 3; 6 amd 12 ppm, (b) Comparison of the Inversion matrix(IM) with the model-predictedFBSD (c) and (d) Comparison between model-calculated IIDDs with experimental measured IIDDs as a function of frother dosages, respectively, PDF and CFD.

Secondly the model was applied against experimental data obtained with different frother concentrations in Mintek pilot plant rougher cell. In this experiment, froth bubble images were not taken in Mintek pilot plant rougher, due to no transparent reactor wall. Only froth bubble size measurements by drop of the probe (Wits Bubble-sizer) were performed. This was used for the validation of the model. Two normal distribution function parameters were employed to model the FBSD. The FBSD for the sample of bubbles were obtained from the IIDD measured employing Wits Bubble-sizer. The two values of parameters for predicting the FBSD were determined by matching the discretized model-predicted IIDD to the discretized experimental measured IIDD using an algorithm model (Figure 5) to find the average and standard deviation optimized in order that the sum square error SSE value be closest to zero. This is the requirement for the completion of fit. With different frother concentrations 3, 6 and 12 ppm, respectively an optimized fitting model parameters (μ, δ) 4.52 and 0.912; 3.55 and 0.651; 2.61 and 0.453 were found to give the SSE values 0.64; 0.54 and 0.24 corresponding to the match between the discretized experimental measured and discretized model IIDD as shown in Figure 9c and 9d. The model-predicted IIDD agrees well with the experimental IIDD in all range of sizes as clearly observed in figure. This is similar compared to the previous laboratory case. A comparison between the discretized FBSD obtained using by least square regression LSR and inversion matrix shown in Figure 9b. As can be seen from Figure, the FBSD obtained with LSR is in agreement with FBSD found through inversion matrix. Figure 7a shows that average diameter and standard deviation of FBSD increase with increasing froth height above the pulp-froth interface, which displays that froth bubble coalescence happens at point to point of froth height FH. While Figure 7b indicates that the average diameter and standard deviation of FBSD increase with decreasing frother dosage. The rate of model parameters are strongly affected by the froth height and frother dosage.

Conclusion

In this work, a probability between the bubble size distribution BSD and intra bubble impact distance distributions IIDD was derived successfully for a single bubble and extended to a population of bubbles with the same spherical shape. This approach provides useful insight into characteristics of IIDDs that can be measured using drop of the probe (Wits Bubble sizer). The stereological techniques to obtain estimates of the actual FBSD from the intra bubble impact distance distribution IIDDs have been developed. The model has been tested successfully. The model was first validated for forth bubbles as a function of froth height. The model was seem to precisely predict the FBSD compared to photographic method. The model was also evaluated for froth bubbles as function of frother concentrations in Mintek pilot plant rougher cells. The model was seen to reasonably predict the FBSD. Froth height and frother dosage seem to have a strong effect on model parameters of FBSD obtained respectively in Wits lab flotation and Mintek pilot rougher cells. Inversion matrix method also estimates FBSD. The present model seems to be simple and does not require more parameters.

Notation

$P(L_b|D_b)$: Cumulative distribution that a random drop of the probe measures an intra bubble impact distance IID having its distance less than or equal to L_j

$p(L_b|D_b)$: Probability density that a random drop of the probe measures an intra bubble impact distance IID having its distance between $L_j \; and \; L_{j+1}$

$p(L_b|D_b)$:

$p\ (D_i)$: Probability density function of bubble size distribution

$p\ (L_j)$: Intra bubble impact distance distributions

L_j: Intra bubble impact distance or chord length

$D_i\ or\ D_b$: Bubble diameter

r_b: Bubble radius

$D_i\ , D_{i+1}$: Boundaries of size class

$L_j\ , L_{j+1}$: Boundaries of intra bubble impact distance class

M: Number of size classes (diameter class)

N: Number of intra bubble impact distance classes

M_i: Number of the bubbles in the i^{th} class

N_j: Number of intra bubble impact distances in i^{th} class

$\overline{D}_i$: Representive size

N_T : Total number of bubbles measured by a probe

μ: Average

δ: Standard deviation

IID (CL): intra bubble impact distance (Chord length)

IIDD: intra bubble impact distance distribution

FBSD: Froth bubble size distribution

BSD: Bubble size distribution

Acknowledgements

Financial support from the Lonmin is gratefully acknowledged. The authors also acknowledge Mintek (South Africa, Johannesburg) for assistance with the measurements of froth bubble sizes in Pilot plant rougher cell using Wits-BubbleSizer.

References

Ata, S., Ahmed, N., Jameson, G.J., 2003. A study of bubble coalescence in flotation froths. Int. J. Miner. Process. 72, 255–266.

Bhondayi, C., Moys, H.M., 2014. Measurement of a proxy for froth bubble sizes as a function of froth depth in flotation machines Part 1. Theoretical development and testing of a new technique. Int. J. Min. Proc., 130, 8-19.

Finch, J.A. Hermandez J.R., Colemen R.G., Gomez C.O., 2004. A comparison between capillary amd imaging technique for sizing bubbles in flotation systems. Min. Eng., 17, 53-61.

Jillavenkatesa, A., Dapkunas, S.J., Lum,L. –S.,2001. Particle size characterization. NIST Special Pub., 1, 960.

Li M., Wilkinson D., 2005. Determination of non-spherical particle size distribution from chord length measurements. Part 1: theoretical analysis. Chem Eng Sci., 60, 3151–3265.

Liu, W., Clark, N.N., 1995. Relationships between distributions of chord lengths and distributions of bubble sizes including their statistical parameters. Int. J. Multiple Flow, 21, 1073.

Liu, J.J., MacGregor, J.F., Duchesne, C., Bartolacci, G., 2005. Flotation froth monitoring using multiresolution multivariate imageanalysis. Min. Eng., 18, 65-76.

Matsuura, A., Fan, L.-S., 1984. Distribution of bubble properties in a gas-liquid-solid fluidized bed. AIChE J.30, 894.

Moys, M.H. and Finch, J.A., 1988. Development in the control of flotation columns. Int. J. Min. Proc., 265-268.

Moys, M.H., 1979. A study of processes occurring in flotation froths. PhD thesis. University of Natal, South Africa.

Murphy, D.G., Zimmerman, W., Woodburn, E.T., 1996. Kinematic model of bubble motion in a flotation froth. Powder technology 78, 3-12.

Seungwoo, P., 2009. Modeling bubble coursing in froth phase from first principles. PhD thesis. State University, USA.

Worlitschek, J., Hocker, T., Mazzotti, M., 2005. Restoration of psd from chord length distributions distribution data using the method of projection onto convex sets. Part. Syst. Charact. 22, 81-98.

Yianatos, J.B., Finch, J.A., Laplante, A.R., 1986. Holdup profile and bubble size distribution of flotation column froths. Canadian Metallurgical Quarterly 25 (1), 23– 29.

Xie, W., Neethling, S.J. and Cilliers, J.J., 2004. A novel approach for estimating the average bubble size for foams flowing in vertical columns. Chemical Engineering Science, Volume 59, issue 1; p. 81-86.

Zhang, W., Nesset, J.E., Kolahdoozan, M., Finch, J.A., 2009. Use of frother for sampling-with-imaging bubble sizing technique. Min. Eng., Vol 22, 413-515